Direct and indirect excitons and magnetic polarons in CdSe/CdMgSe/CdMnSe semimagnetic double quantum wells

I. I. Reshina,* S. V. Ivanov, D. N. Mirlin, I. V. Sedova, and S. V. Sorokin
Ioffe Physical-Technical Institute RAS, 194021 St. Petersburg, Russia
(Received 3 August 2006; revised manuscript received 18 September 2006; published 22 December 2006)

We have studied exciton photoluminescence and reflection spectra as well as formation of localized magnetic polarons and spin tunneling in CdSe/CdMgSe/CdMnSe asymmetric double quantum well structures with different barrier thicknesses. Measurements were performed in strong magnetic fields both in Faraday and Voigt configurations. Direct excitons from nonmagnetic CdSe and semimagnetic CdMnSe quantum wells were observed, as well as a spatially indirect exciton formed by the electron in the CdSe quantum well and the heavy hole in the CdMnSe one. The problem of the direct and indirect exciton forming localized magnetic polarons is addressed. Polarization properties of direct and indirect excitons are studied. In the case of a thin barrier, spin tunneling is observed under magnetic field. Calculations of the exciton energies are performed. The calculated values are found to be in reasonable agreement with the measured ones.

DOI: 10.1103/PhysRevB.74.235324 PACS number(s): 78.55.Et, 78.67.De, 71.35.−y, 75.75.+a

I. INTRODUCTION

Asymmetric double quantum wells (ADQW) providing a possibility to study direct and indirect excitons and their tunneling properties have received a great deal of attention due to fundamental scientific significance and device applications.[1–8] Recently, diluted magnetic ADQW have attracted interest in the growing field of spintronics.[9–13]

In the present work, we have studied spectra of exciton photoluminescence (PL), photoluminescence excitation (PLE) and reflection as well as excitons tunneling in ADQW structures with CdSe and CdMnSe quantum wells and CdMgSe barriers of different thickness. Formation of localized magnetic polarons has been studied. We have recently studied PL and vertical transport of charge carriers and excitons of CdSe/CdMgSe superlattices with various periods.[14] The tunneling properties of excitons (including spin tunneling) in semimagnetic ADQW can be controlled both by the barrier thickness and energy level tuning by an applied magnetic field. We observed direct and indirect excitons and were primarily interested in the properties of the latter under strong magnetic fields applied in Faraday and Voigt configurations.

II. EXPERIMENT

Four CdSe/$Cd_{1-x}Mg_xSe$/$Cd_{1-y}Mn_ySe$ ADQW structures, whose parameters are given in Table I, were grown by molecular beam epitaxy (MBE) on InAs (001) substrates, passivated previously in a Na_2S solution. The III-V and II-VI MBE growth chambers were connected via an ultrahigh vacuum transfer module. The InAs substrates were sequentially annealed at up to 480 °C until a pronounced (2×4) reconstruction of the surface was attained under an As_4 flux. Then the substrates were transported into the II-VI growth chamber, where the growth of the CdMgSe compounds was initiated in the epitaxy mode with an enhanced atomic migration.[15] A 0.3 μm-thick CdMgSe layer was grown at 280 °C, followed by five periods of the CdSe/CdMgSe/CdMnSe ADQW structures separated from each other by approximately 10 nm-thick CdMgSe barriers. Finally, a 0.1 μm-thick CdMgSe layer and a 5 nm-thick CdSe cap layer were grown. The surface conditions during growth were monitored by reflection high-energy electron diffraction, demonstrating clear (2×1) Se stabilized surface reconstruction. The widths of the layers and the average Mg and Mn concentrations were determined by x-ray diffraction measurements and the growth rate calibrations. The widths of the layers were also measured directly by transmission electron microscopy (TEM). Measurements of PL and reflection spectra were made with the use of a pumped He cryostat with a superconducting solenoid. Magnetic fields up to $B=7$ T in Faraday or Voigt configuration could be applied.

TABLE I. Parameters of the ADQW structures used in this work.

Sample no.	CdSe width	$CdMn_xSe$ width	$CdMg_ySe$ coupling barrier width	$CdMg_ySe$ wide barrier width	Mn concentr.	Mg concentr.
	11, nm	l2, nm	d, nm	D, nm	x	y
1-309	3.8	3.4	1.2	6.7	0.073	0.20
1-307	4.2	4.0	3.0	6.3	0.073	0.20
1-371	4.4	4.05	5.1	9.7	0.065	0.17
1-373	4.1	5.9	5.2	10.0	0.065	0.15
1-372[a]		3.8		9.7	0.065	0.17

[a]Single QW.

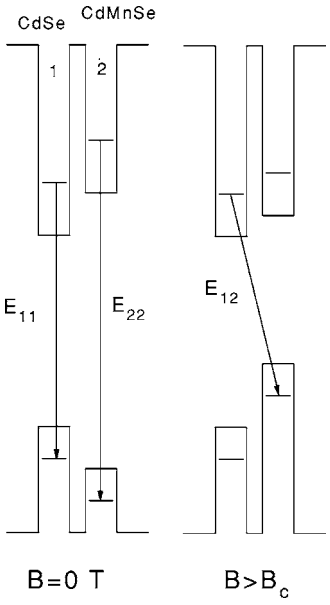

FIG. 1. Scheme of the potential of ADQW for σ^+ polarization at $B=0$ T and at high B values.

The sample was in contact with cold He vapor. The spectra were recorded by using a computer-controlled grating spectrometer with a double monochromator and photon counting electronics. He-Ne, Kr^+, and Ar^+ lasers were employed for PL excitation. PLE spectra and selective PL were measured under excitation by a halogen lamp via a single grating monochromator. The halogen lamp was also used for measurement of the reflection spectra.

III. THEORETICAL BACKGROUND

Conduction and valence band lineup of the ADQW under σ^+ polarization at zero magnetic field and at a large magnetic field, and the observed optical transitions are shown schematically in Fig. 1. Due to exchange interaction between carriers (electrons and holes) and manganese ions under magnetic field applied in the Faraday configuration ($\vec{B}$ along the growth axis), there is a very large splitting between spin levels of the conduction and valence bands of the semimagnetic quantum well (SQW). The direct heavy-hole exciton of the SQW has a $|-\frac{1}{2},\frac{3}{2}\rangle$ ground state and its energy decreases with B.[16] The shift of the energy as a function of the magnetic field B is described by the well-known relation[17]

$$\Delta E = \Delta E_c + \Delta E_v = -\frac{1}{2}[x_{eff} N_0(\alpha+\beta)\langle S_z^{\mathrm{Mn}}\rangle], \qquad (1)$$

where x_{eff} is the effective concentration of Mn^{2+} which is lower than the total Mn^{2+} concentration due to formation of Mn pairs with antiferromagnetic interaction, $N_0(\alpha+\beta)$ is the sum of the exchange integrals for the conduction and valence bands, and $\langle S_z^{\mathrm{Mn}}\rangle$ is the thermal average of the Mn spin projections along $\vec{B}$, given by the modified Brillouin function B_S for $S=5/2$,

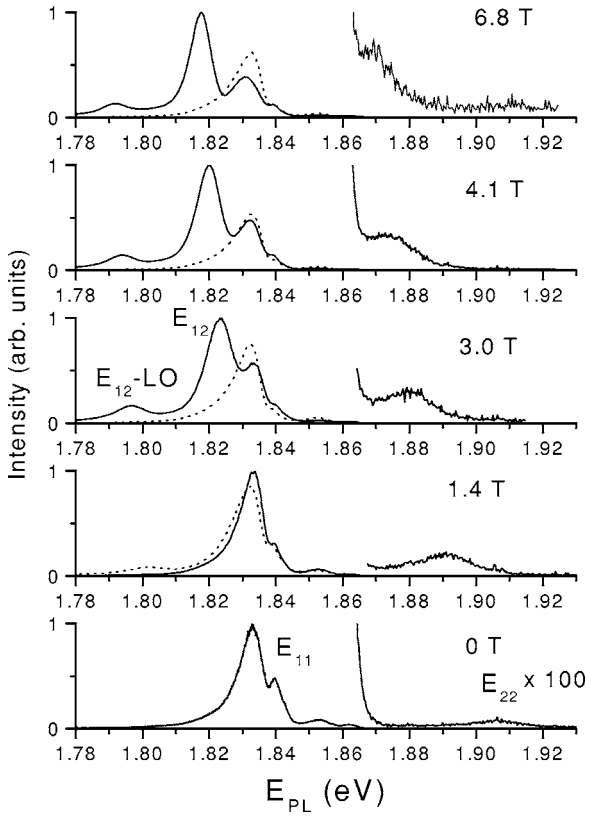

FIG. 2. PL spectra of ADQW 1-307 at different magnetic fields. Excitation at 1.96 eV. PL intensity of the E_{22} peak from the SQW is increased by a factor of 100. Spectra for σ^- polarization are shown by dotted curves.

$$\langle S_z^{\mathrm{Mn}}\rangle = -(5/2)B_{5/2}\left[\frac{5\mu_B B}{k_B(T+T_{AF})}\right], \qquad (2)$$

where μ_B is the Bohr magneton, k_B is the Bolzmann constant, T is the temperature, and T_{AF} is the parameter due to antiferromagnetic pairing of Mn^{2+} ions. Equations (1) and (2) have two adjustable parameters, x_{eff} and T_{AF}.

Two indirect exciton transitions may also exist in the ADQW: (i) electron level in the nonmagnetic CdSe well (NQW) and heavy-hole level $J=3/2$ in the SQW, (ii) electron $S=-1/2$ level in the SQW and the heavy-hole level in the NQW. All magnetic splittings and shifts excluding those caused by exchange interaction can be neglected. In the Voigt configuration ($\vec{B}$ parallel to the sample plane) the splitting of the conduction band does not change, whereas there exists a large anisotropy of exchange interaction for the valence band and the splitting of the heavy-hole band is very small.[18,19]

IV. EXPERIMENTAL RESULTS AND DISCUSSION

A. Faraday configuration

PL spectra of sample 1-307 at different magnetic fields in the Faraday configuration under σ^+ and σ^- polarization are presented in Fig. 2. PL was excited at 1.96 eV (higher than the SQW exciton transition). At $B=0$ T the most intense line

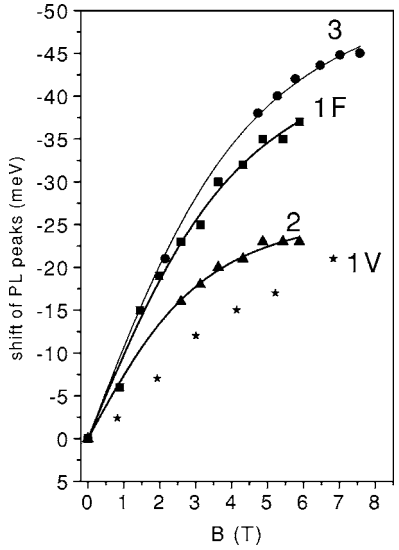

FIG. 3. ADQW 1-307. Magnetic shifts of the E_{22} exciton in the Faraday (curve 1F) and the Voigt (curve 1V) configurations and of the E_{12} exciton in Faraday configuration (curve 2 without accounting for LMP formation, curve 3 for B_P=2.1 T).

is the direct donor-bound heavy-hole exciton D^0X of the NQW at 1.835 eV. The line on its high-energy shoulder E_{11} is probably due to the quasi-free exciton X (localized by quantum well thickness fluctuations). The line E_{22} at 1.91 eV is the direct heavy-hole exciton of the SQW. It is three orders of magnitude weaker than the D^0X line in the NQW because of fast carrier and exciton tunneling to the NQW. As B increases, the line E_{22} moves to lower energies and at 6.8 T merges with the tail of the exciton lines in the NQW. This shift, as already mentioned, is due to the exchange splitting of the conduction and heavy-hole valence bands of the SQW in the magnetic field. Figure 3 shows the experimental data for this shift and their fit with Eqs. (1) and (2) (curve 1F). Bulk values of the exchange integrals $N_0\alpha$=258 meV and $N_0\beta$=|1110|meV,[20] were used. We have obtained from the fit x_{eff}=0.028 and $T+T_{AF}$=7.8 K.

Let us return to Fig. 2. At B=3 T, a different band and its LO (CdSe)-phonon replica are seen on the low-energy side of the D^0X exciton of the NQW. Actually, this band already appears at the field of 1.45 T as indicated by the appearance of its phonon replica. But the band itself is merged with the D^0X band. As the magnetic field increases, this band shifts to lower energies and becomes the most intense one in the spectrum. We believe that this band is due to the spatially indirect heavy-hole exciton (E_{12}) formed by the electron in the NQW and the heavy hole in the SQW. The experimental evidence for such interpretation will be given below. The shift of the E_{12} peak with the magnetic field is caused by the shift of the SQW valence band only. In order to find the experimental shift of the E_{12} peak, its position at B=0 T was estimated by polynomial extrapolation of its position under various values under magnetic field. From the fit of the E_{12} shift, we obtained a 1.5 times smaller effective concentration of Mn^{2+} than from the shift of the E_{22} line, namely x_{eff}=0.019 (curve 2 in Fig. 3). Such discrepancy may be caused, at least partly, by formation of localized magnetic polarons and will be discussed below. Figure 4 presents for sample 1-307 the magnetic field dependences of energy positions of all excitonic peaks observed in the PL spectra under σ^+ polarization. Figure 5 shows these dependences for excitonic peaks seen in reflection spectra under σ^+ and σ^- polarization. The peaks corresponding to the indirect exciton were not observed in the reflection spectra most likely due to their small oscillator strength typical for indirect excitons. The positions of the direct heavy-hole and light-hole excitons of the NQW do not depend on B up to 7 T. As seen in Fig. 2, the exciton peak E_{12} and its phonon replica are fully σ^+ polarized already at comparatively small magnetic fields, as well as the direct exciton E_{22} of the SQW. These polarization properties show that the E_{12} peak is linked to the SQW. The direct exciton peak of the NQW has a small σ^- polarization.

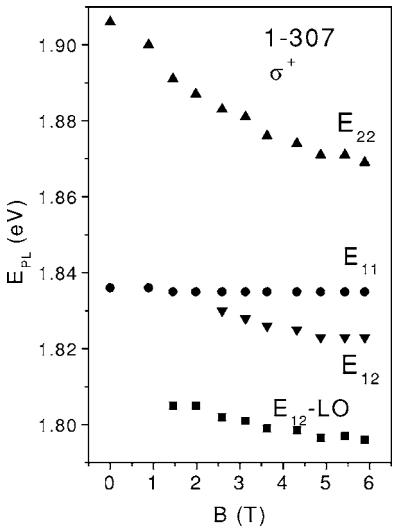

FIG. 4. Positions of excitons observed in σ^+-polarized PL versus magnetic field. ADQW 1-307. (E_{12}-LO labels the phonon replica of the indirect exciton E_{12}.)

The PL spectra of three samples, with nominally the same well width and different barrier thicknesses are compared in

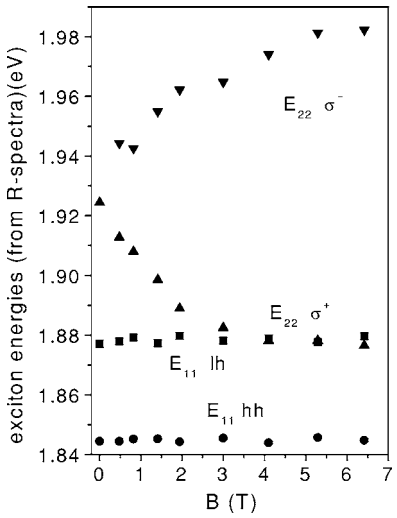

FIG. 5. Positions of excitons observed in σ^+- and σ^--polarized reflection spectra. ADQW 1-307.

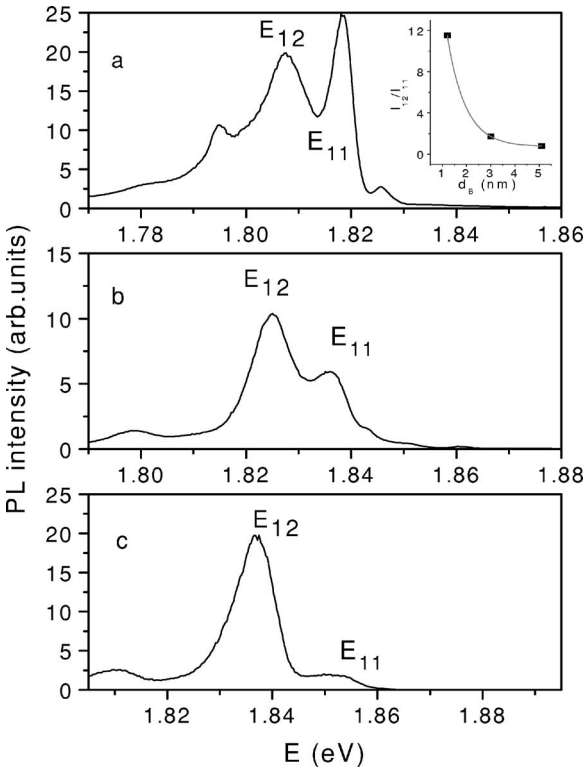

FIG. 6. PL spectra of three ADQW's with different barrier thickness: (a) 5.1 nm, (b) 3.0 nm, (c) 1.2 nm. σ^+ polarization, B=4.3 T. The inset shows the relative intensity of the E_{12} and E_{11} peaks as a function of the barrier thickness d_B.

Fig. 6. For the sample with the smallest barrier thickness of only 1.2 nm [Fig. 6(c)], the E_{22} peak of the SQW is five orders of magnitude weaker than the donor-bound exciton peak of the NQW. This is due to the highest tunneling probability for this sample. The indirect peak of this sample is the strongest as compared to the intensity of the donor-bound exciton peak of the NQW, as is seen in the inset to Fig. 6. The growth of the E_{12} peak intensity is related to the larger overlap of the electron and heavy-hole wave functions with decreasing barrier thickness.

The intensity of the indirect peak increases strongly with the increase of the magnetic field and its half-width begins to decrease at B=3.5 T, as shown in Fig. 7.

The spectrum of sample 1-373 has a peculiar look (Fig. 8). Whereas in other samples the phonon replicas of the E_{12} peak have a smaller intensity than the zero-phonon peak, in sample 1-373 the first phonon replica becomes stronger in intensity than the E_{12} peak when magnetic field increases and is also much broader, as seen in Fig. 8. The peculiarity of the spectrum of this sample is at present unclear. The shifts in the magnetic field of the E_{12} peak and its first phonon replica are seen in the lower panel of Fig. 8.

B. Voigt configuration

In the Voigt configuration, the direct and indirect exciton lines were observed in the linear $\pi\sigma$ polarization, where π is parallel and σ perpendicular to the magnetic field. The shifts

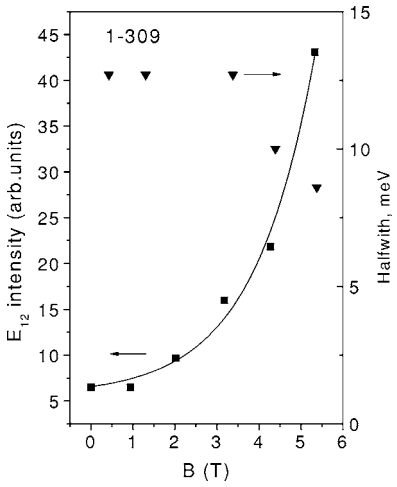

FIG. 7. PL intensity and half-width of the indirect exciton peak E_{12} as a function of magnetic field. ADQW 1-309.

of the direct and indirect exciton lines versus magnetic field were much smaller than in the Faraday configuration, due obviously to the small exchange splitting of the heavy-hole band. The magnetic shift of the direct exciton line E_{22} in the SQW of sample 1-307 in Voigt configuration is shown in Fig. 3 (curve 1V). The shift of the indirect exciton line in the range 2.5–6.9 T was found to be only 3 meV. This again shows that the indirect exciton is associated with the heavy-hole band of the SQW.

C. Spin tunneling

As was already mentioned, the direct exciton line in SQW and the indirect exciton and its phonon replicas are fully σ^+ polarized even at comparatively low magnetic fields, due to strong exchange splitting of the spin-up and spin-down

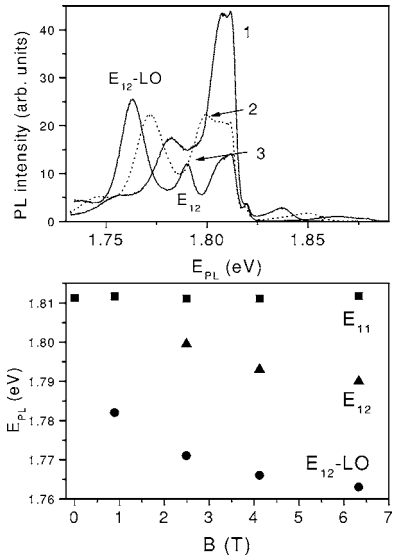

FIG. 8. PL spectra of ADQW 1-373 at different magnetic fields (1–0.9, 2–2.5, 3–6.3 T); the arrows indicate the E_{12} peak. On the lower panel, exciton energy is shown as a function of the magnetic field.

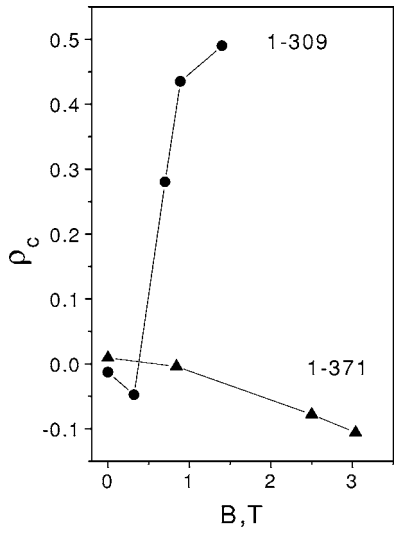

FIG. 9. Circular polarization of the E_{11} exciton as a function of magnetic field for ADQW's with different barrier thickness.

levels in the SQW. Polarization behavior of the direct excitons in the NQW is more complicated. Let us note that the lines of the D^0X and E_{11} excitons and the indirect exciton are overlapped at small B, and in order to find the line intensities and their polarization one has first to deconvolute the spectra measured in σ^+ and σ^- polarization into individual lines. Carriers and excitons tunneling from the SQW contribute to the PL from the NQW, as is revealed from the PL and PL excitation spectra. The tunneling probability in ADQW increases exponentially with decreasing barrier thickness. Degree of circular polarization, ρ_c, of the direct NQW exciton under magnetic field shows a different behavior in samples with different barrier thickness, see Fig. 9. In sample 1-309 with a 1.2 nm-thick barrier, ρ_c is negative at small B, as should be expected (in the NQW the ground exciton state $|+\frac{1}{2}.-\frac{3}{2}\rangle$ is active in the σ^- polarization), but ρ_c becomes positive and increases at larger B. This can be explained by the tunneling of σ^+-polarized excitons from the SQW and population inversion in the NQW. By contrast, in sample 1-371 with a 5.1 nm-thick barrier, ρ_c is continuously negative at all B values and its absolute value increases with B.

D. Formation of localized magnetic polarons

As was mentioned in Sec. IV A, different values of effective Mn^{2+} concentration, x_{eff}, which were found from magnetic shifts of peaks E_{12} and E_{22} may be due, at least partly, to formation of localized magnetic polarons.[21] The exciton magnetic polarons are formed due to polarization of magnetic ion spins by the exchange field B_p of the holes, which play a dominant role in the exchange interaction with magnetic ions.[22] In this case, the carrier energy is suppressed by the so-called polaron energy E_p, or polaron shift. Polaron shift is related to the polaron exchange field B_p, as

$$B_p = \left.\frac{2E_p}{d\varepsilon_F/dB}\right|_{B=0}, \tag{3}$$

where ε_F is the heavy hole splitting under magnetic field in Faraday geometry.[23] If the magnetic polaron is formed, the shift of the PL peak occurs in the total field

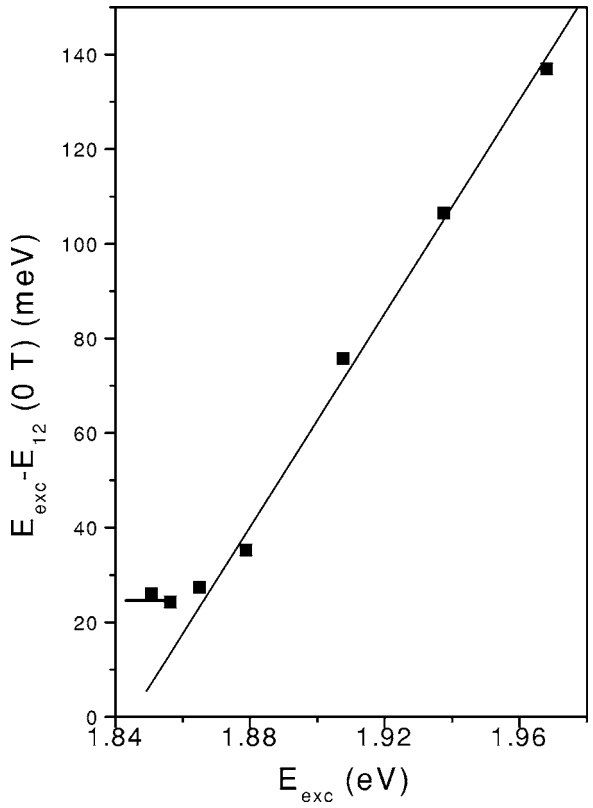

FIG. 10. $E_{exc}-E_{12}$ as a function of E_{exc} at nonselective and selective excitation. E_P is marked by a horizontal line.

$$B_{total} = B_{external} + B_p. \tag{4}$$

In order to verify the formation of the localized magnetic polarons, two methods can be applied. In the first method, E_p is found directly by PL measurements under selective excitation in the region of localized exciton states.[21] We applied this method for the indirect exciton E_{12}. The results for sample 1-307 are shown in Fig. 10. In this case we estimate E_p=25 meV, $B_p \approx 2.15$ T and get $x_{eff} \approx 0.03$ as distinct from the value 0.019 when formation of the magnetic polaron was not taken into account. These values correspond evidently to magnetic polaron in thermal equilibrium because of a long lifetime of the indirect exciton. Figure 11 explains how we take into account the exchange field B_p and obtain values for the shifts of the E_{12} peak. These shifts and the fit by Eq. (1) are shown in curve 3 of Fig. 3. We could not apply the selective excitation method to the E_{22} peak because its intensity is very small due to tunneling of excitons into the NQW. Thus we have applied the second method,[24] where E_p can be found from the derivative of the circular polarization ρ_c with respect to B at small magnetic fields.

$$E_p = \left.\frac{1}{2\pi k_B T}\left[\frac{dE_z/dB}{d\rho/dB}\right]^2\right|_{B=0}, \tag{5}$$

and

$$B_p = \left.\frac{dE_z/dB}{\pi k_B T (d\rho/dB)^2}\right|_{B=0}, \tag{6}$$

where E_z is the magnetic splitting of the heavy-hole exciton.[23] We have found for the E_{22} peak of sample 1-307

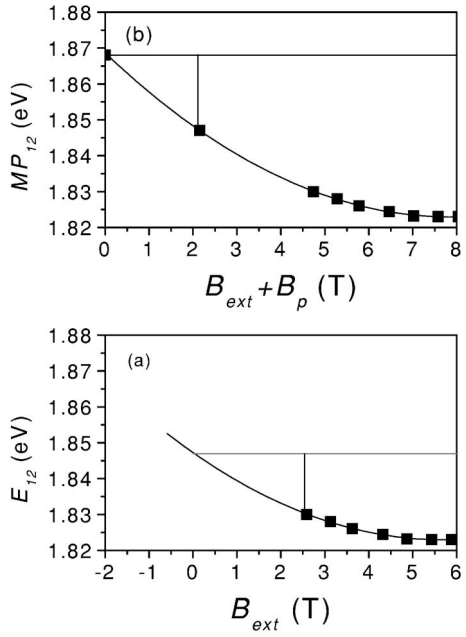

FIG. 11. ADQW 1-307. (a) E_{12} energy versus external magnetic field B_{ext}. (b) Replotted E_{12} energy versus the total magnetic field, $B_{ext}+B_P$. The exchange magnetic field $B_P=2.1$ T. The shifts from the $E_{12}(B=0$ T) value are indicated by vertical lines and shown in Fig. 3.

$E_p=2$ meV and $B_p=0.14$ T. Thus, we conclude that for the E_{22} exciton the process of magnetic polaron formation is interrupted due to a short lifetime and tunneling time of the E_{22} exciton in samples with a small barrier thickness. The shift of E_{22} is shown by curve 1F in Fig. 3 and it runs very close to curve 3.

Now we would like to mention that the decrease of the half-width of the E_{12} peak with B (Fig. 7) could be related to its magnetic polaron nature. We observed such an effect also for the magnetic polaron peak of a single semimagnetic quantum well CdMnSe/CdMgSe. Earlier, such an effect was also observed for a single quantum dot CdMnTe/CdMgTe and related to the kinetics of magnetic polaron formation, i.e. the transient shift of the emission line during the magnetic polaron formation time.[25]

For sample 1-373 with a 5.1 nm-thick barrier, we obtained close values of E_p (26 and 32 meV) for E_{12} and E_{22} peaks, respectively, by the two methods discussed. Thus, for a sample with a thicker barrier, both excitons are forming localized magnetic polarons.

V. CALCULATIONS OF INTERBAND TRANSITIONS AND EXCITON BINDING ENERGIES

Calculations of interband transition energies of the ADQW structures and envelope wave functions were performed by a transfer matrix method[26,27] with or without accounting for deformation. The physical parameters are given in Table II. The band gap of the semimagnetic well was taken from the measurements of the CdMnSe bulk layers grown by MBE with the same concentration of Mn as in the ADQW. We have used an experimentally derived equation[28] for E_G of the $Cd_{1-x}Mg_xSe$ barriers:

$$E_G = xE_G(\mathrm{MgSe}) + (1-x)E_G(\mathrm{CdSe}) - Cx(1-x), \quad (7)$$

where $C=0.2$, $E_G(\mathrm{CdSe})=1.765$ eV, and $E_G(\mathrm{MgSe})=4.05$ eV.

The values for lattice constants and elastic stiffness constants of $Cd_{1-x}Mg_xSe$ were calculated via a linear interpolation between the values for CdSe and MgSe. The values of

TABLE II. Physical parameters of CdSe and MgSe used in the calculations of interband transitions of ADQW structures.

	CdSe	MgSe	InAs
a_0(Å)	6.077	5.89	6.0583
C_{11} (Nm^{-2})	6.67×10^{10}[a]	9.8×10^{10}[b]	
C_{12} (Nm^{-2})	4.63×10^{10}[a]	6.27×10^{10}[b]	
a (eV)	−3.664[a]		
a_c (eV)	−2.625[a]		
b (eV)	−0.8[a]		
m_e/m_0	0.11[d]		
m_{hh}/m_0	0.45[d]		
m_{lh}/m_0	0.145[d]		
E_G (eV) at 2 K	1.765[c]	4.05[b]	
Δ_0 (eV)	0.42[e]		
ε	9.53[f]		

[a]Reference 30.
[b]Reference 28.
[c]Reference 31.
[d]Reference 32.
[e]Reference 33.
[f]Reference 34.

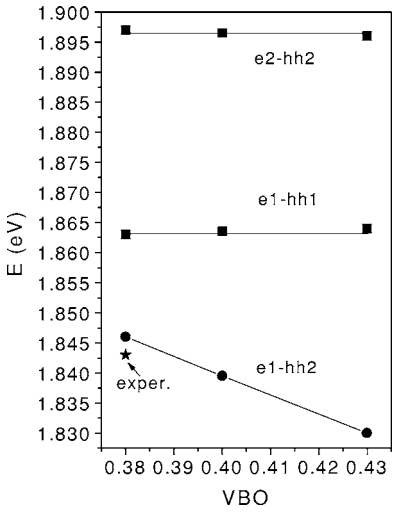

FIG. 12. Calculated energies (symbols) of the interband transitions as a function of relative valence band offset (VBO) of the CdMnSe well. VBO of the CdSe well is taken equal to 0.35. Solid lines are guides for the eye. The experimental point for the E_{12} peak is shown by an asterisk.

TABLE III. Measured and calculated exciton energies and exciton binding energies E_B for sample 1-307.

	$B=0$ T			$B=5.9$ T			
Exciton transition	Measured (eV)	Calculated interband transition (eV)	Calculated exciton energy (eV)	Measured (eV)	Calculated interband transition (eV)	Calculated exciton energy (eV)	Calculated E_B (meV)
E_{11} (CdSe)	1.845	1.862	1.838	1.845	1.863	1.840	22.8
E_{22} (CdMnSe)	1.924	1.940	1.919	1.877	1.897	1.876	21.0
E_{12}		1.881	1.872	1.823[a]	1.846	1.838	8.2

[a]From PL measurements. The usual Stokes shift 0.01 eV has to be added for comparison with the calculated results.

the effective mass in the barriers were determined as the values in the well multiplied by the ratio of the band gaps of the barrier to the well. Since the values of the hydrostatic and the shear deformation potentials for MgSe are not known and Mg concentration did not exceed 20%, we used the same values as for CdSe. For the interface of CdSe and CdMgSe, a relative-valence band offset (VBO) of 0.35 was used. The VBO for the CdMnSe/CdMgSe interface is not known, but can be found from the position of the indirect exciton peak. Let us note that whereas energies of direct interband transitions depend only weakly on the VBO, the energies of the indirect transitions have a very strong nearly linear dependence on VBO, as can be seen in Fig. 12. Let us note that position of the E_{12} peak depends slightly on the incident power density of the exciting light probably due to built-in electric fields. However, in sample 1-307, the shift was only 1 meV when the incident power density was changed by an order of magnitude. Therefore we have used the energy of the indirect exciton in this sample to estimate the VBO for the CdMnSe/CdMgSe interface and have found VBO=0.38.

We can use the experimentally obtained shift of the E_{22} exciton in the Faraday configuration, decompose it into the conduction and valence band shifts using the known bulk values of the exchange integrals, add the found shifts to the conduction and valence bands potentials at $B=0$ T and obtain zone edge positions corresponding to a particular magnetic field, as shown schematically in Fig. 1. Account for deformation resulted in very small changes of *e-hh* transition energies (within 1 meV). Exciton binding energy, E_B, was calculated from Eq. (24) of Leavitt and Little.[29] The experimental and calculated results for exciton energies for sample 1-307 are presented in Table III and we find them to be in reasonable accordance.

VI. CONCLUSION

In conclusion, we have studied exciton photoluminescence and reflection spectra of cubic asymmetric double quantum well structures CdSe/CdMgSe/CdMnSe grown by MBE pseudomorphically on InAs (001). Measurements were performed in magnetic fields up to 7 T both in Faraday and Voigt configurations. Gigantic splitting of spin levels in the diluted magnetic quantum well resulted in circular polarization of the exciton peaks related to this quantum well and allowed energy level tuning. We focused on the properties of the spatially indirect exciton, which was shown to be formed by the electron in the nonmagnetic CdSe quantum well and the heavy hole in the semimagnetic one. In Faraday geometry, the indirect exciton became the lowest energy state of the structure at magnetic fields around 1.5–2 T. It was fully $\sigma+$ polarized and had up to two phonon replicas. As magnetic field increased, the position of the indirect exciton shifted to lower energies, its intensity strongly increased, and the half-width decreased. The problem of localized magnetic polarons formation was studied. The nature of the indirect exciton state as a localized magnetic polaron was established. It was shown that in structures with a thin coupling barrier, the direct exciton of the SQW does not form a localized magnetic polaron, due to fast tunneling into the NQW. The efficiency of the exciton and spin tunneling from the SQW to the NQW was studied as a function of the barrier thickness. The relative valence band offset of CdMnSe/CdMgSe interface was estimated using the sensitivity of the indirect exciton position to VBO. Calculations of exciton energies were made and found to be in reasonable accordance with the experimental values.

ACKNOWLEDGMENTS

The authors are very thankful to K. V. Kavokin for fruitful discussions and A. A. Sitnikova for TEM measurements. This work was partly supported by the Russian Foundation for Basic Research, Grant No. 06-02-16245 and the Program of RAS on Spintronics.

*Email address: reshina@dnm.ioffe.rssi.ru

[1] F. Capasso, K. Mohammed, and A. Y. Cho, IEEE J. Quantum Electron. **22**, 1853 (1986).
[2] J. E. Golub, K. Kash, J. P. Harbison, and L. T. Florez, Phys. Rev. B **41**, 8564 (1990).
[3] A. Alexandrou, J. A. Kash, E. E. Mendez, M. Zachau, J. M. Hong, T. Fukuzawa, and Y. Hase, Phys. Rev. B **42**, 9225 (1990).
[4] I. Lawrence, S. Haacke, H. Mariette, W. W. Rühle, H. Ulmer-Tuffigo, J. Cibert, and G. Feuillet, Phys. Rev. Lett. **73**, 2131 (1994).
[5] F. C. Michl, R. Winkler, and U. Rössler, Solid State Commun. **99**, 13 (1996).
[6] W. Heimbrodt, L. Gridneva, M. Happ, N. Hoffmann, M. Rabe, and F. Henneberger, Phys. Rev. B **58**, 1162 (1998).
[7] K. Kayanuma, E. Shirado, M. C. Debnath, I. Souma, S. Permogorov, and Y. Oka, Physica E (Amsterdam) **10**, 295 (2001).
[8] G. N. Aliev, J. Puls, L. Parthier, F. Henneberger, and W. Heimbrodt, Physica E (Amsterdam) **10**, 511 (2001).
[9] S. Lee, M. Dobrowolska, J. K. Furdyna, H. Luo, and L. R. Ram-Mohan, Phys. Rev. B **54**, 16939 (1996).
[10] S. Lee, G. Yang, M. Dobrowolska, and J. K. Furdyna, J. Korean Phys. Soc. **39**, 447 (2001).
[11] I. A. Buyanova, W. M. Chen, B. Monemar, A. A. Toropov, Ya. V. Terent'ev, S. V. Sorokin, A. V. Lebedev, S. V. Ivanov, and P. S. Kop'ev, Physica E (Amsterdam) **13**, 538 (2002).
[12] M. Poggio, G. M. Steeves, R. C. Myers, N. P. Stern, A. C. Gossard, and D. D. Awschalom, Phys. Rev. B **70**, 121305(R) (2004).
[13] S. Lee, M. Dobrowolska, and J. K. Furdyna, Physica E (Amsterdam) **26**, 271 (2005).
[14] I. I. Reshina, S. V. Ivanov, D. N. Mirlin, I. V. Sedova, and S. V. Sorokin, Fiz. Tekh. Poluprovodn. (S.-Peterburg) **39**, 456 (2005) [Semiconductors **39**, 432 (2005)]; Phys. Status Solidi C **3**, 1143 (2006).
[15] S. V. Ivanov, O. G. Lyublinskaya, Yu. B. Vasilyev, V. A. Kaygorodow, S. V. Sorokin, I. V. Sedova, V. A. Solov'ev, B. Ya. Meltser, A. A. Sitnikova, T. V. L'vova, V. L. Berkovits, A. A. Toropov, and P. S. Kop'ev, Appl. Phys. Lett. **84**, 4777 (2004).
[16] J. K. Furdyna, J. Appl. Phys. **64**, R29 (1988).
[17] J. A. Gaj, R. Planel, and G. Fishman, Solid State Commun. **29**, 435 (1979).
[18] P. Peyla, A. Wasiela, Y. Merle d'Aubigné, D. E. Ashenford, and B. Lunn, Phys. Rev. B **47**, 3783 (1993).
[19] B. Kuhn-Heinrich and W. Ossau, Mater. Sci. Forum **182–184**, 491 (1995).
[20] D. Heiman, in *12th International Conference on High Magnetic Fields in the Physics of Semiconductors, Würzburg, Germany, 1996*, edited by G. Landwehr and W. Ossau (World Scientific, Singapore, 1997), Vol. 2, p. 847.
[21] G. Mackh, W. Ossau, D. R. Yakovlev, A. Waag, G. Landwehr, R. Hellmann, and E. O. Göbel, Phys. Rev. B **49**, 10248 (1994).
[22] K. V. Kavokin, I. A. Merkulov, D. R. Yakovlev, W. Ossau, and G. Landwehr, Phys. Rev. B **60**, 16499 (1999).
[23] I. A. Merkulov, D. R. Yakovlev, K. V. Kavokin, G. Mackh, W. Ossau, A. Waag, and G. Landwehr, Pis'ma Zh. Eksp. Teor. Fiz. **62**, 313 (1995) [JETP Lett. **62**, 335 (1995)].
[24] I. A. Merkulov, G. R. Pozina, D. Coquillat, N. Paganotto, J. Siviniant, J. P. Lascaray, and J. Cibert, Phys. Rev. B **54**, 5727 (1996).
[25] A. A. Maksimov, G. Bacher, A. McDonald, V. D. Kulakovskii, A. Forchel, C. R. Becker, G. Landwehr, and L. Molenkamp, Phys. Rev. B **62**, R7767 (2000).
[26] L. R. Ram-Mohan, K. H. Yoo, and R. L. Aggarwal, Phys. Rev. B **38**, 6151 (1988).
[27] R. Pérez-Álvarez, C. Trallero-Herrero, and F. Garcia-Moliner, Eur. J. Phys. **22**, 275 (2001).
[28] V. A. Kaygorodov, V. S. Sorokin, I. V. Sedova, O. V. Nekrutkina, S. V. Sorokin, T. V. Shubina, A. A. Toropov, and S. V. Ivanov, Acta Phys. Pol. A **100**, 443 (2001).
[29] R. P. Leavitt and J. W. Little, Phys. Rev. B **42**, 11774 (1990).
[30] Yi-Hong Wu, IEEE J. Quantum Electron. **30**, 1562 (1994).
[31] C. Guenaud, E. Deleporte, A. Filoramo, Ph. Lelong, C. Delalande, C. Morhain, E. Tournie, and J. P. Faurie, J. Cryst. Growth **184-185**, 839 (1998).
[32] V. Pellegrini, R. Atanasov, A. Tredicucci, F. Beltram, C. Amzulini, L. Sorba, L. Vanzetti, and A. Franciosi, Phys. Rev. B **51**, 5171 (1995).
[33] C. G. Van de Walle, Phys. Rev. B **39**, 1871 (1989).
[34] R. G. Alonso, E.-K. Suh, A. K. Ramdas, N. Samarth, H. Luo, and J. K. Furdyna, Phys. Rev. B **40**, 3720 (1989).